I_h is an unlikely primary cause of increased excitability in axotomised Aα/β-fibre neuronal somata.

Chaplan SR et al. (2003) J Neurosci 23: 1169-1178.

Tu H et al. (2004) J Neurosci Res 76: 713-722.

Yao H et al. (2003) J Neurosci 23: 2069-2074.

This work was supported by a Wellcome Trust UK grant to S.N.L. and PhD scholarship from the University of Bristol.

Authors have confirmed where relevant, that experiments on animals and man were conducted in accordance with national and/or local ethical requirements.

C77

Background light modulates activated rhodopsin lifetime in mouse rods

C. Chen[1], M.L. Woodruff[2], F.S. Chen[1], D. Chen[3] and G.L. Fain[2,4]

[1]Biochemistry and Molecular Biology, Virginia Commonwealth University, Richmond, VA, USA, [2]Physiological Science, UCLA, Los Angeles, CA, USA, [3]Tulane University, New Orleans, LA, USA and [4]Ophthalmology, UCLA, Los Angeles, CA, USA

Retinal rods adapt to steady background light by acceleration of response decay and a decrease in sensitivity. Recent experiments (1) have shown that in mouse, response decay quickens largely from modulation of turn-off of cyclic GMP phosphodiesterase (PDE). This process also decreases sensitivity, but experiments on salamander rods suggest that a Ca-dependent change in activated rhodopsin (R*) lifetime may also make an important contribution (2). Changes in R* lifetime are difficult to study directly, since it is normally so short that PDE turnoff is rate limiting for the decay of the light response. We therefore made suction-electrode recordings from isolated rods (as in ref. 1) of mice genetically engineered to make PDE turnoff much more rapid than normal, and R* turnoff slower, so that rod responses would decay only as R* activity was extinguished. We used R9AP95 mice in which the GTPase activating (GAP) proteins are over-expressed by about 6-fold. Since the GAP proteins are obligate activators of transducin alpha GTP hydrolysis, they regulate the rate of PDE turnoff, and overexpression of these proteins greatly speeds the kinetics of PDE deactivation (3). We then mated the R9AP95 mice with animals in which rhodopsin kinase (RK) activity had been reduced either to about 40% (in RK+/-) or about 15% (in RKux), in order to slow the rate of rhodopsin phosphorylation and turnoff of R*. We quantified the rate of turnoff by fitting the waveform of response recovery to a single exponential with time constant τ_REC. Previous experiments showed that τ_REC in animals that are R9AP95 alone is less than 80 ms and much more rapid than in WT animals (3), indicating that R9AP95 alone greatly accelerates PDE turnoff, which is normally rate-limiting. The value of τ_REC, however, was progressively slowed to 112 ± 16 (SE, n = 14) in R9AP95;RK+/- and 415 ± 70 (n = 7) in R9AP95;RKux. This shows that decreasing rhodopsin kinase activity with RK+/- and RKux slows the rate of rhodopsin phosphorylation sufficiently, so that R* lifetime becomes rate-limiting for response decay. When these rods were then exposed to background light, flash response recovery was accelerated. This could only have occurred if the R* lifetime was shortened by the background. This is the first direct physiological demonstration that R* lifetime is modulated during light adaptation. Our results also indicate that response recovery can be accelerated even in the absence of a background simply by increasing the flash intensity. Since increasing intensities produce progressively larger and longer reductions in circulating current and decreases in outer segment Ca, our results are consistent with a mechanism in which background light lowers Ca, which in turn decreases R* lifetime probably by modulating the rate of rhodopsin phosphorylation.

Woodruff ML et al. (2008). J Neurosci 28, 2064 2074.

Matthews HR (1996). J Physiol 490, 1 15.

Krispel CM et al. (2006). Neuron 51, 409 416.

Supported by NIH grants EY13811 and EY01844 to CKC and GLF.

Authors have confirmed where relevant, that experiments on animals and man were conducted in accordance with national and/or local ethical requirements.

C78

Odor learning under anaesthesia: behavioural, neurochemical and electrophysiological effects

A. Nicol[1], G. Sanchez-Andrade[1], H. Fischer[1], P. Collado[2], A. Segonds-Pichon[1] and K. Kendrick[1]

[1]Babraham Institute, Cambridge, UK and [2]Cd Universitaria, Madrid, UK

Carbon disulphide (CS_2) in the exhaled breath of rodents increases the attractiveness of food odours. Thus information about foods which are safe to eat is transmitted between individuals. When one individual smells a food odour on the breath of another, it eats more of that food than it would otherwise. Here we investigate this system of odour learning in anaesthetised mice.

Food odours were prepared by mixing the ingredient with normal feed, and introducing the altered food in non-airtight capsules into gas-sampling bags containing N_2. Bags were also prepared with CS_2 (10μM), or the unaltered feed, both in N_2. Mice were anaesthetised with isofluorane in 21% N_2 and 79% O_2. Stimuli were delivered by switching from this supply to a matched supply carrying a food odour and/or CS_2. In experiment 1, Mice were trained by exposure to a novel food odour combined with CS_2 for 60s, then allowed to recover from anaesthesia. Controls were exposed to a novel food odour alone, or to CS_2 alone. When tested 24h after odour exposure, food preference was biased towards an odour that had been presented with CS_2 during anaesthesia.

In experiment 2, mice were anaesthetised and a microelectrode array (6x4 tungsten electrodes, tip separation 350μ) was positioned in the OB. Action potentials (spikes) were sampled from neurons in the mitral cell layer of the OB (≤8 neu-

rons per electrode). Ten second presentations were made of the plain food odor, and the odors of food with ginger or coriander added: ~10 trials per odor with 5min inter trial intervals. Ten presentations were then made of the ginger food odor combined with CS_2. In subsequent tests with the altered and plain food odors, neuronal responsiveness was biased towards the training odor relative to either of the other two odors.

In experiment 3, mice were anaesthetised and trained by nose to nose contact with an anaesthetised mouse which had consumed a novel flavoured food (trained group), or plain food (control group). When tested 24h after odour exposure, food preference again reflected odour exposure during anaesthesia. Immediately after testing, the mice were re-anaesthetised, and neurochemical samples were collected from the OB by microdialysis during three consecutive 1min deliveries of the flavoured or plain food. In animals trained with flavoured food odour during anaesthesia, presentation of the flavoured food odour, but not the plain food odour, produced an increase in glutamate (142.5%±20.4SEM), GABA (155.3%±19.2) and noradrenaline (137.3%±28.4) in the OB. This was not so in animals exposed only to plain food odour under anaesthesia.

These experiments demonstrate that this system of odour learning functions effectively in anaesthetised mice exposed to an artificial mix of food odour with CS_2. Neurochemical changes and altered OB neuronal responsiveness also reflect odour exposure during anaesthesia.

Authors have confirmed where relevant, that experiments on animals and man were conducted in accordance with national and/or local ethical requirements.

C79

Cortex-muscle oscillatory interactions show a developmental profile in humans

L.M. James[2,3], J.A. Stephens[3], D.M. Halliday[4] and S.F. Farmer[1,2]

[1]Department of Neurology, Institute of Neurology, London, UK, [2]Department of Clinical Neurophysiology, Imperial College Healthcare NHS Trust, London, UK, [3]Department of Physiology, University College London, London, UK and [4]Department of Electronics, University of York, York, UK

In adult humans, coherence and cumulant analysis of the Electroencephalogram (EEG) and Electromyogram (EMG) shows that frequency components within the scalp EEG and contralateral EMG are coupled at approximately 20 Hz, during the performance of motor tasks requiring voluntary isometric muscle contraction (Halliday et al., 1998).

Analysis of EMG recordings between steadily co-contracting synergistic hand muscles shows that there is significant coupling at ~20Hz frequencies. This EMG-EMG coupling has been attributed to central nervous system oscillatory drive and it has been shown to have a developmental profile with increasing levels as subjects reach adolescence (Farmer et al., 2007). Beta (~20 Hz) frequencies in the EEG increase around the time of adolescence (Gasser et al., 1988). Given this latter finding it is of interest to know whether the direct interaction between rhythmical elements comprising the EEG over the motor cortex and the contralateral EMG might also change with increasing age.

With ethical approval, simultaneous recordings of EEG and rectified surface EMG recordings from forearm extensor muscles were obtained from 48 subjects aged between 0-59 years during a sustained right wrist extension motor task. The techniques of EEG-EMG coherence and cumulant analysis (Halliday et al., 1998) and pooled coherence and cumulant analysis (Amjad et al., 1997) were used to analyze the EEG and EMG signals. Data collected from different age groups were compared.

Subjects within age groups 0-3 years and 4-10 years did not demonstrate both significant (P<0.05) coherence and cumulant. Within the age range of 12-17 years 30% of the subjects demonstrated both signficant (P<0.05) coherence and cumulant between left motor cortex EEG and right arm EMG. For Adults within the age range 19-55 years, 46% of subjects showed both significant (P<0.05) coherence and cumulant between left motor cortex EEG and right arm EMG. Comparisons made using a chi squared test across all four age groupings showed significant differences between children under the age of 10 years and the adult subjects (P = 0.036).

These results demonstrate a significant effect of age on corticospinal oscillatory interaction as measured by EEG-EMG coherence and cumulant density estimates.

The results show for the first time that changes in the cortical ~ 20 Hz oscillatory drive to human motoneurone pools take place during motor development in man.

The relatively late emergence of ~20 Hz EEG-EMG coherence in humans, may reflect an important developmental change in the central nervous system, with implications for central nervous system plasticity and motor control.

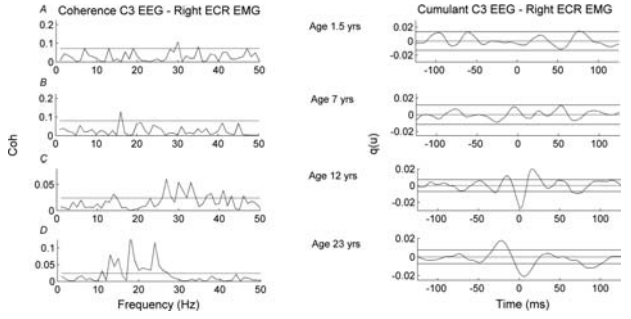

Coherence and cumulant between left motor cortex EEG and right forarm extensor EMG in 4 subjects of different ages. The data show the emergence in the older subjects of ~20 Hz coherence with associated triphasic cumulant.

Amjad AM et al. (1997). J Neurosci Methods 73, 69-79.

Farmer SF et al. (2007). J Physiol 579, 389-402.

Gasser T et al. (1988). Electroenceph Clin Neurophysiol 69, 91-99.

Halliday DM et al.(1998). Neurosci Lett 241, 5-8.

Authors have confirmed where relevant, that experiments on animals and man were conducted in accordance with national and/or local ethical requirements.

Male Wistar rats (n=8, 275-350g) were anaesthetised (Ketamine 60mg.kg-1/Medetomidine 25μg.kg^{-1} i.p.) and injected stereotaxically into the IO (n=7) and/or GN (n=8) with mixtures of anterograde (fluoro-ruby or fluoro-emerald) and retrograde tracers (red or green fluorescent latex microspheres). In all but 1 case, successful injections were made into both sites in the same animal. After 5-7 days survival, animals were terminally anaesthetised (propofol, 30mg.kg.h^{-1} i.v.), perfusion fixed, and brains and dorsal root ganglia (DRG) removed for histological processing. In 40μm sections, injection sites in the medulla and retrogradely labelled neurones in the PAG, and in L5 DRG were mapped with a fluorescence microscope and plotted onto representative transverse sections. Anterograde terminal labelling in the cerebellum and retrogradely labelled neurones in the DRG were used to confirm the position of injection sites in IO and GN respectively.

In the same animal, injections into IO resulted in a significantly higher number of labelled cells, as compared to GN (olive=80±10; gracile=20±6; mean±SEM; t-test, p<0.0001). IO injections resulted in labelled neurones throughout the PAG with significantly more in the DL/L-PAG as opposed to VL-PAG (t-test, p<0.01). Additionally, significantly more labelled neurones were identified in caudal PAG compared to rostral PAG (caudal=108±8; rostral=53±4; mean±SEM; t-test, p<0.01).

The current data raise the possibility that neurones in the PAG may modify motor behaviour by modulating olivocerebellar (climbing fibre) pathways. That columnar (including rostrocaudal) differences in the organisation of these projections may underlie the different motor responses co-ordinated by the PAG requires further investigation.

LOVICK, TA and BANDLER, R (2005) The organisation of the midbrain periaqueductal grey and the integration of pain behaviours. In: SP Hunt and M Koltzenburg eds. The Neurobiology of Pain. Oxford University Press, Oxford, UK. Ch 11

This work is funded by a grant from the BBSRC and Charlotte Flavell is funded by the MRC

Authors have confirmed where relevant, that experiments on animals and man were conducted in accordance with national and/or local ethical requirements.

PC101

The role of glutamate receptor ligands in allodynia, hypersensitivity and morphine analgesia during neuropathic pain in mice

M. Osikowicz, J. Mika, W. Makuch and B. Przewlocka

Department of Pain Pharmacology, Institute of Pharmacology, Polish Academy of Sciences, Krakow, Poland

Recent evidence have indicated that metabotropic glutamate receptor (mGluR) type 5, 2/3 and 7 are present in regions of central nervous system important for nociceptive transmission [2-4], but their involvement in neuropathic pain has not been well established. The present study was aimed to exam the influences of mGluR5 antagonist: MPEP, mGluR2/3 agonist: LY379268 and mGluR7 agonist: AMN082 on development of neuropathic pain symptoms and on morphine effects in Albino Swiss mice after sciatic nerve injury. Chronic constriction injury (CCI) to the sciatic nerve was performed under pentobarbital (36 mg/kg; I.P.) anaesthesia using the procedure described by Bennett and Xie [1]. The mechanical allodynia (von Frey test) was performed in order to evaluate sensitivity to mechanical stimulus. The cold plate test was used to assess sensitivity to cold stimulus. The experimental procedures were performed according to the Institute's Animal Research Bioethics Committee and in accordance with the NIH Guide for the Care and Use of Laboratory Animals. The data were calculated as the mean ± SEM or as a percent of maximal possible effect (%MPE) ± SEM (n=8-12 per group). Our results demonstrated that both acute and chronic administration of MPEP, LY379268, and AMN082 attenuated allodynia and hyperalgesia seven days after CCI in mice. Moreover, single administration of MPEP (30 mg/kg; I.P.) or LY379268 (10 mg/kg; I.P.) injected 30 min before morphine (20 mg/kg; I.P.) potentiated morphine analgesic effect towards mechanical allodynia and thermal hyperalgesia in the mouse CCI model. Whereas, a single administration of AMN082 (3 mg/kg; I.P.) potentiated the effects of a single morphine injection (20 mg/kg; I.P.) only in the von Frey test. Chronic administration (for seven days) of low doses of MPEP, LY379268 or AMN082 (all drugs at 3 mg/kg; I.P.) potentiated the effects of single doses of morphine (3, 10, 20 mg/kg; I.P.) administered on the last day of experiment; however, AMN082 potentiated only the effect in the cold plate test. Additionally, the same doses of MPEP and LY379268 (but not AMN082) chronically co-administered with morphine (40 mg/kg; I.P.) attenuated the development of morphine tolerance in CCI-exposed mice [5, in press, PAIN]. Our data suggests that mGluR5, mGluR2/3, and mGluR7 are involved in injury-induced plastic changes in nociceptive pathways and that mGluR5 and mGluR2/3 ligands enhanced morphine's effectiveness in neuropathy, which could have therapeutic implications.

Bennett GJ, Xie YK (1988). Pain 33, 87-107

Bhave G et al. (2001). Nat Neurosci 4, 417-423.

Carlton SM et al. (2001). Neuroscience 105, 957-969.

Li H et al. (1997). Neurosci Lett 223, 153-156.

Osikowicz M et al. (2008). Pain, in press.

Supported by statutory funds of the Institute of Pharmacology PAS.

Authors have confirmed where relevant, that experiments on animals and man were conducted in accordance with national and/or local ethical requirements.

PC102

Serotonin-specific reuptake inhibitors (SSRI) blunt bitter taste acutely (minutes), but enhance it chronically (hours) in normal healthy humans

S. O'Driscoll, E. McRobie, C. Ayres, N. Mileusnic, T.P. Heath, J.K. Melichar and L.F. Donaldson

Physiology and Pharmacology, University of Bristol, Bristol, UK

Serotonin is postulated to act as either a transmitter between taste cells and gustatory neurones, and/or as an intercellular signal, modulating taste transmission within the taste bud itself

(1). Systemic SSRIs affect human taste thresholds, lowering bitter and sweet recognition thresholds while not affecting salt thresholds (2) 2 hours after administration.
Bitter and salt recognition thresholds were determined in up to 26 healthy volunteers (age range 19-47;13 male,13 female) at the tip of the tongue at each of four experimental sessions. Different concentrations of bitter (quinine) and salt (NaCl) solutions were presented to each subject in a pseudorandom order, using cotton buds soaked in each solution. Each taste concentration was presented a minimum of 5 times before and after drug or placebo in each of two experiments (double-blind). Psychophysical taste functions were constructed to calculate bitter and salt taste threshold for each volunteer and intervention. Expt. 1 (n=21) Taste thresholds determined before and 15 minutes after a 5 minute application of either SSRI (Seroxat™ elixir, 2mg/ml) or placebo (proprietary cough mixture) application to the lingual epithelium. Both drugs were citrus flavoured. Expt. 2 Taste thresholds determined before, 30 minutes (n=11) and 2 hours (n=26) after systemic paroxetine (20mg) or inactive placebo. Data shown are mean ±SEM.
Expt 1. Lingually applied SSRI resulted in an increase in bitter recognition threshold (threshold after – threshold before) of 54±34%, which was significantly greater than the change after placebo (-39±26%; p=0.03 paired t test). The net effect of SSRI (ΔSSRI-Δplacebo) was to increase thresholds by 27±18μM. The changes in salt threshold after lingual SSRI were not significantly different from those after placebo (-44±25% SSRI, -54±23% placebo; p=0.8 paired t test).
Expt 2. Systemic SSRI tended to increase bitter thresholds at 30 minutes (ΔSSRI-Δplacebo, +17±29%). This small increase in threshold at 30 minutes was significantly different from the decrease in bitter threshold at 2 hours reported previously (-32±22%, p=0.02, Wilcoxon)(2). There was no significant effect of systemic SSRI on salt thresholds at any time.
These data suggest that acute inhibition of 5-HT reuptake at the taste bud blunts bitter taste (increases thresholds) whereas chronic inhibition (2 hours) enhances bitter taste (decreases thresholds). This difference may represent a difference in the site of action of 5-HT (taste bud or CNS), or a temporal effect of acute (minutes) versus chronic (hours) reuptake inhibition.

Roper SD (2006).*Cell.Mol.Life Sci.***63**,1494-1500

Heath TP *et al (2006).* J. Neurosci.***26(49)**,12664-12671*

This work was funded by the Dept of Physiology and Pharmacology, UoB.

Authors have confirmed where relevant, that experiments on animals and man were conducted in accordance with national and/or local ethical requirements.

PC103

Biophysical model of *Drosophila* photoreceptor

Z. Song[1,2], D. Coca[1], S. Billings[1] and M. Juusola[2]

[1]Department of Automatic Control and System Engineering, University of Sheffield, Sheffield, UK and [2]Department of Biomedical Science, University of Sheffield, Sheffield, UK

To gain understanding how complex bio-molecular interactions govern the conversion of light stimuli into voltage responses in the fly eye, we generated a simplified biophysical model of a *Drosophila* photoreceptor that included photo-sensitive and photo-insensitive membrane.
Photoreceptors transform images falling on the eyes into electrical signals and transmit that information toward the brain for updating neural representations of the visual world. Unlike in mammalian retina, where rods and cones are specialized for dim and bright vision, respectively, *Drosophila* photoreceptors can reliably transform the combined range of nocturnal and diurnal intensity changes into electrical responses(1). However, relatively little is known about dynamic interactions that enable such a powerful adaptation. By constructing a mathematical model of a Drosophila photoreceptor, based on experimentally measured parameters, we aim to learn more how feedback interactions within and between the photo-sensitive and photo-insensitive membrane provide the necessary gain control mechanisms for light-adaptation.
It is believed that photo-transduction cascade, which translates light-quanta into light current (i.e. trans-membrane current-responses), happens mainly in the photo-sensitive part (rhadomere) of fly photoreceptors, whereas the photo-insensitive membrane helps to convert light current into a well-defined voltage response. Accordingly, there are two parts in our model. The dynamics of light current are simulated by a simplified cascade model of the known biochemical interactions within rhadomere, giving rise to realistic light current responses. These signals then drive a model of the photo-insensitive cell body, which uses Hodgkin-Huxley-formalism to approximate the dynamics of the known voltage-gated ion-channels(2).
In order to understand the relative roles of the different parts in the phototransduction cascade, our model of photo-sensitive membrane has a simplified structure. It contains only first order linear differential equations and static nonlinearities, whereupon complicated responses to different inputs are regulated by feedback loops - believed to be the key mechanisms of optimal adaptation.
The combined model is validated by performing intracellular measurements from *Drosophila* photoreceptors to light stimuli *in vivo* and by comparing these to the model output for similar inputs. Even in this relatively basic form, our model can predict well the waveforms of voltage responses to simple light inputs. From a practical and systemic point of view, this model can now serve as a preprocessing module for high-order models of the *Drosophila* visual system that we intend to build due course.

1. Hardie, R.C. & Raghu, P. (2001). Nature 41:186-193.

2. Niven, J.E., Vähäsöyrinki, M., Kauranen, M., Hardie, R.C., Juusola, M., & Weckström, M. (2003). Nature 421: 630-634.

We thank Roger Hardie for discussions and providing key parameters for the model. This research is funded by the University of Sheffield, the BBSRC, the EPSRC and the Gatsby Foundation.

Authors have confirmed where relevant, that experiments on animals and man were conducted in accordance with national and/or local ethical requirements.

PC104

Regional variation in glutamate taste recognition thresholds on the human tongue

L.F. Donaldson, L. Bennett, L. Rooshenas, B. Feakins, E.K. Richardson, N. Jones, C. Kenyon, V. Smith, S. Raichura and J.K. Melichar

Physiology and Pharmacology, University of Bristol, Bristol, UK

Many textbooks continue to publish the human tongue map, in which specific regions of the tongue are denoted as being the area in which the four basic tastes, salt, sour, sweet and bitter, are detected, despite the fact that this map was shown to be incorrect 30 years ago (1). Although there are regional differences in sensitivity for detection of different taste modalities on the tongue, in general the four well-known taste modalities can be detected in all areas of the tongue, in addition to the soft palate and oropharynx. Taste recognition is also related to age in that in the elderly population, taste generally becomes blunted with increasing age. Much less is known about the fifth taste, umami, the taste of glutamate. In this study we have investigated possible regional variations in sensitivity for glutamate taste detection across the human tongue, and the relationships between glutamate recognition threshold and 1) age, and 2) perception of taste intensity.

Monosodium glutamate (MSG) recognition thresholds were determined in 34 healthy volunteers (age range 19-71; 6 male 28 female) at the tip (n=34), the sides (n=7) and the back (n=19) of the tongue. Solutions of MSG ranging in concentration from ~180mM to ~300μM were applied to each region of the tongue, each concentration a minimum of 5 times. Subjects indicated whether or not they could recognise the taste stimulus at each concentration. MSG thresholds were calculated for each region using psychophysical taste function curves. Taste intensity of a supra-threshold stimulus (1M) was measured using a 150mm generalised labelled magnitude scale anchored at "barely detectable" and "strongest imaginable sensation of any kind". Data shown are mean ± SEM.

The back and sides of the human tongue had similar MSG recognition thresholds, with only slight differences between the regions (back, 14±3mM; left, 25±9mM; right 26±10mM; ns; Kruskal Wallis + Dunn's post-hoc). The MSG recognition threshold at the tip of the tongue was significantly greater than that at the back of the tongue (tip, 60±13mM, $p<0.01$, Dunn's) than the tip of the tongue. There was no relationship between age and MSG threshold, but there was a significant negative correlation between MSG threshold and intensity ratings ($p=0.03$, $r=-0.4$, $n=30$, Spearman rank correlation).

There is no significant drop in MSG sensitivity with increasing age in young/middle aged adults. The perceived intensity of MSG taste is related to the recognition threshold - the lower the threshold, the more intense the taste. There are regional differences in MSG taste threshold across the human tongue, but MSG could be tasted in all regions tested. The greatest difference in MSG recognition thresholds exists between the tip and the back of the tongue.

Collings, V. (1974). *Perception and Psychophysics* **16(1)**, 169-174.

This work was supported by the Dept of Physiology and Pharmacology, University of Bristol.

Authors have confirmed where relevant, that experiments on animals and man were conducted in accordance with national and/or local ethical requirements.

PC105

Distribution of Cx45 expression throughout the murine spinal cord

R.J. Chapman[1], A.E. King[1], S. Maxeiner[2], K. Willecke[2] and J. Deuchars[1]

[1]Institute of Membrane and Systems Biology, University of Leeds, Leeds, UK and [2]Division of Molecular Genetics, University of Bonn, Bonn, Germany

Gap junctions are clusters of connexin containing channels that are expressed in regions of apposing membranes in coupled cells (Evans & Martin, 2002). Characterisation of connexin expression within the CNS is vital to the ultimate functional understanding of gap junctions. To date, there are ~20 known isoforms of connexin proteins and about half of mammalian connexins are expressed in the central nervous system (Willecke *et al.*, 2002). Additionally, the neuronal connexin subtype, Cx45, has been found in α-motorneurons of the spinal ventral horn using *in situ* hybridization (Chang *et al.*, 1999). Using Cx45-reporter mice expressing GFP (Maxeiner *et al.*, 2003), we aimed to characterise the distribution of GFP-positive cells throughout the adult mouse spinal cord.

<P>Animals anaesthetised deeply with sagatal (60mg.kg ip) were perfused trans-cardially with 4% paraformaldehyde in 0.1M phosphate buffer (pH 7.4) and the spinal cords harvested. All procedures accord with the UK Animals (Scientific Procedures) Act 1986. 50μm transverse sections were cut of both thoracic and lumbar spinal cord. Sections were then incubated in either mouse anti-NeuN (1:1000, Chemicon) or mouse anti-GFAP (1:1000, Affinity) or biotinylated IB4 (1:100, Vector Labs), and chicken anti-GFP (1:1000, Invitrogen) at 4ºC for 12-36hrs. Anti-GFP was then visualised using $Alexa^{488}$-conjugated donkey anti-chicken (1:1000, Invitrogen). NeuN and GFAP were individually visualised using $Alexa^{555}$-conjugated donkey anti-mouse (1:1000, Invitrogen), and IB4 visualised with Strepdavidin $Alexa^{555}$ (1:100, Invitrogen).

<P>The distribution of GFP-expressing cells was highly concentrated within laminae II/III in both thoracic and lumbar spinal dorsal horn (DH), with a few cells noted in lamina I. No cells expressing GFP were observed in the spinal ventral horn (cf. Chang *et al.*, 1999). The total number of cells expressing GFP in the lumbar DH was significantly higher than in the thoracic spinal DH (22.6±0.7 cells lumbar and 17.8±0.7 cells thoracic; *t*-test, $P<0.001$, $n=3$), and the number of cells expressed per $10\mu m^2$ was also significantly higher (3.17±0.1 cells lumbar and 2.76±0.07 cells thoracic; *t*-test, $P<0.05$, $n=3$). Staining with isolectin B4 (IB4) revealed that GFP expressing cells within lamina III received close appositions from fibers originating from laminae I/II. The post-mitotic neuronal marker, NeuN, was found to co-localise with presumed Cx45-immunopositive neurons in the spinal DH laminae, but no co-localisation was observed with the glial fibrillary acidic protein, GFAP.

<P>These data suggest a highly localised expression of this connexin protein which may potentially play a significant role in the processing of somatosensory and sensorimotor afferent

information. Further studies are now required to determine the DH cell type expressing this Cx45 protein.

Chang *et al.*, 1999, J. Neurosci. 19(24):10813-10828.

Evans & Martin, 2002, Mol. Memb. Biol. 19:121-136.

Maxeiner *et al.*, 2003, Neuroscience 119(3):689-700.

Willecke *et al.*, 2002, Biol. Chem. 383(5):725-737.

This work was supported by The Wellcome Trust.

Authors have confirmed where relevant, that experiments on animals and man were conducted in accordance with national and/or local ethical requirements.

PC106

Human cone photopigment regeneration assessed using the electroretinogram: slower recovery following intense bleaches

O.A. Mahroo[1] and T.D. Lamb[2]

[1]Physiology, Development & Neuroscience, University of Cambridge, Cambridge, UK and [2]John Curtin School of Medical Research and ARC Centre of Excellence in Vision Science, Australian National University, Canberra, ACT, Australia

Photopigment regeneration after bleaching can reveal much about retinal function in health and disease. Recently a "rate-limited" model has been proposed, whereby 11-*cis* retinal diffuses into photoreceptor outer segments through a resistive barrier from a constant pool in the pigment epithelium, resulting in regeneration proceeding linearly with time rather than as an exponential (Lamb & Pugh, 2004; Mahroo & Lamb, 2004). We tested this hypothesis for cone pigment regeneration following very intense bleaches, posing two questions. Does regeneration follow a linear rate after intense bleaches? If so, is the rate the same as for smaller bleaches, as the model predicts? We used a conductive fibre electrode to record electroretinogram photopic *a*-wave responses to red flashes (0.4 photopic cd m^{-2} s) following one-minute bleaching exposures (11 000 - 130 000 photopic cd m^{-2}) in two normal subjects with dilated pupils. A blue background (40 scotopic cd m^{-2}), present throughout, eliminated rod signals. Post-bleach response amplitudes were used to estimate pigment regeneration using a transformation published previously (Mahroo & Lamb 2004). Recoveries proceeded according to a linear rate: first order exponentials gave strikingly poorer fits than the "rate-limited" model (see Fig. 1). However, the rate was around 30% slower than that obtained previously from the same subjects following less intense bleaches (Mahroo & Lamb, 2004), suggesting that the model needs modification.

Cone pigment appears to regenerate more slowly following very intense bleaches. This may indicate a reduction in the 11-*cis* retinal pool available, shedding new light on retinal mechanisms after exposure to intense illumination.

Figure 1. Cone pigment recovery following intense bleach

Fifteen dim red flashes (0.40 cd m^{-2} s at 0.5 s intervals) were presented every 10 s after 1 min exposure to yellow light of 40,000 photopic cd m^{-2}. Response amplitudes, measured 14-15 ms after each flash, were used to estimate pigment level (Mahroo & Lamb, 2004, Eqn (9) and (10)). Points plot mean ± S.E.M, over 20 s windows, with results from six exposures, so each point averages c.180 flash presentations. Panels fit recovery for a 100% bleach with different models: points differ slightly between panels as fits give different estimated dark-adapted amplitudes, affecting normalization.

A, Curve shows best-fitting form of recovery as a single exponential, with time constant of 2.2 min.

B, Solid curve: best-fitting recovery according to rate-limited model, giving parameters K_m = 0.2 and rate v = 0.33 min^{-1}. Dashed curve: expected recovery if v is 0.5 min^{-1}, which fitted recoveries in this subject from less intense exposures (Mahroo & Lamb, 2004).

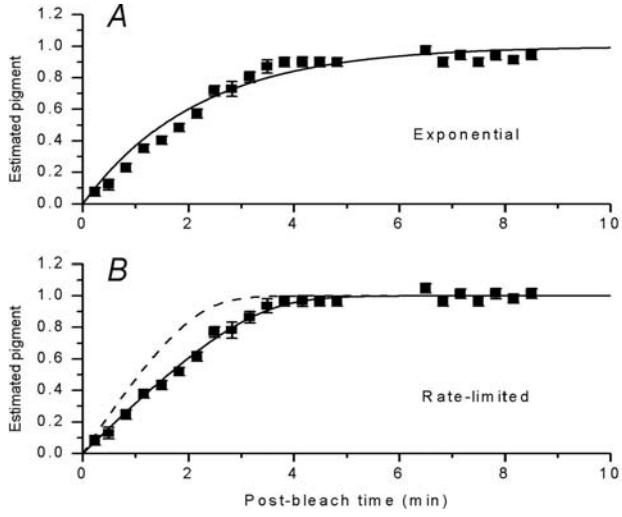

Figure 1

Lamb & Pugh (2004). *Progress in Retinal and Eye Research* **23,** 307-80.

Mahroo & Lamb (2004). *Journal of Physiology* **554,** 417-37.

MSD Studentship to OARM, ARC Federation Fellowship FF0344672 to TDL.

Authors have confirmed where relevant, that experiments on animals and man were conducted in accordance with national and/or local ethical requirements.

PC107

Levetiracetam inhibits calcium signalling in cultured dorsal root ganglia neurons from neonatal rats

M. Ozcan[1], E. Alcin[2], S. Kutlu[2] and A. Ayar[2]

[1]Biophysics, Firat University, Medical School, Elazig, Turkey and [2]Physiology, Firat University Faculty of Medicine, Elazig, Turkey

Although the novel antiepileptic drug levetiracetam (LEV) have been shown to be effective in the treatment of pain, the mechanisms mediating its antinociceptive actions are still not well understood. The aim of this study was to investigate the effects of LEV on Ca2+ transients, evoked by high-K+ (30 mM) in cultured rat dorsal root ganglion (DRG) neurons. DRG neuronal cultures were loaded with 5 μmol Fura-2 AM and Ca2+ responses to stimulation with high-K+ were assessed by using the fluorescent ratiometry. Fura-2 loaded DRG cultures were excited at 340 and 380 nm, and emission was recorded at 510

nm by using imaging system consisting of CCD camera coupled to an inverted microscope with a 40x (1.30 NA S Fluor, Oil) objective. High-K+ responses were determined by the change in 340/380 ratio (basal-peak) and the area under the fluorescence ratio-time curve (AUC) was also calculated for individual DRG neurons in selected microscopic fields. All data were analyzed by using an unpaired t test, with a 2-tailed P level of <.05 defining statistical significance. LEV dose-dependently reduced the [Ca2+]i increase, elicited by 30 mM KCl, in a reversible manner. The mean 340/380 nm ratio was 1.18±0.06 (baseline, n=17), 1.15±0.06 (30 μM LEV, P>0.05, n=17) and 1.17±0.05 (recovery, n=17); 1.28±0.04 (baseline, n=17), 1.14±0.03 (100 μM LEV, P>0.05, n=17) and 1. 28±0.03 (recovery, n=17); 1.21±0.03 (baseline, n=18), 1.08±0.02 (300 μM LEV, P>0.05, n=18), and 1.21±0.02 (recovery, n=18), respectively. The AUC changes were consistent with the mean ratio results; the effects of 100 and 300 μM LEV being significant. Our results indicate that LEV significantly suppressed depolarisation-induced intracellular calcium changes in a dose-dependent fashion in dorsal root ganglion neurons. The inhibition of calcium signals in these sensory neurons by levetiracetam might contribute to the antinociceptive effects of the drug.

Keywords: Levetiracetam; dorsal root ganglia, fluorescence calcium imaging, pain, sensory neurons

The authors wish to thank to UCB Pharma for generously providing Levetiracetam (ucb LO59).

Authors have confirmed where relevant, that experiments on animals and man were conducted in accordance with national and/or local ethical requirements.

PC108

Effects of essential hypertension on short latency human somatosensory evoked potentials

L. Edwards[1], C. Ring[1], D. McIntyre[1], U. Martin[2] and J.B. Winer[3]

[1]School of Sport & Exercise Sciences, University of Birmingham, Birmingham, UK, [2]School of Medicine, University of Birmingham, Birmingham, UK and [3]Neurology, University Hospital Birmingham, Birmingham, UK

Reduced sensitivity to peripheral nerve stimulation in hypertension may be explained by subclinical axonal neuropathy of sensory afferents (Edwards *et al.* 2008). The current study aimed to further explore this phenomenon by investigating whether the ascending somatosensory pathway is affected by hypertension. Following ethical approval and in accordance with the Declaration of Helsinki, we examined the peripheral median nerve N9, spinal N13 and cortical N20 short latency somatosensory evoked potentials (sSEPs) in 14 patients with unmedicated essential hypertension (9 men, 40 ± 6 years; mean ± sd) and 22 normotensive volunteers (10 men, 37 ± 6 years). The sSEPs were elicited by 100 μs electrocutaneous stimulation of the median nerve at the wrist for 2000 trials (Mauguiere *et al.* 1999). A series of 2 Group (hypertensive, normotensive) ANCOVAs were performed on sSEP amplitudes and latencies, with age and arm length as covariates. N9 amplitudes were significantly reduced (*P*<.01) in hypertensives (3.60 ± 1.26 μV) compared to normotensives (5.71 ± 2.24 μV). In contrast, N20 amplitudes were not different between hypertensives (4.38 ± 2.35 μV) and normotensives (3.87 ± 2.20 μV). Furthermore, none of the sSEP latencies differed between groups: N9 (hypertensives: 10.21 ± 0.78 ms, normotensives: 10.36 ± 0.76 ms), N13 (hypertensives: 13.33 ± 0.99 ms, normotensives: 13.57 ± 0.98 ms) and N20 (hypertensives: 19.23 ± 1.26 ms, normotensives: 19.35 ± 0.95 ms). In addition, a 2 Group (hypertensive, normotensive) ANCOVA, with age as a covariate, performed on the sensory median nerve conduction velocity, revealed no differences between hypertensives (61.46 ± 3.77 m/s) and normotensives (61.27 ± 3.63 m/s). Two hierarchical regression analyses were conducted to determine the association between N9 amplitude and 24-hour ambulatory systolic and diastolic blood pressures while accounting for confounding by age and stimulation-to-recording distance. N9 amplitudes were inversely associated with systolic (*P*<.01) and diastolic (*P*<.05) blood pressure. As the amplitude of a sensory action potential reflects the number of large diameter myelinated fibres synchronously depolarised in the vicinity of the active recording electrode (Buchthal & Rosenfalck, 1966), a reduction may indicate axonal loss (Gilliatt, 1978). As N9 amplitudes, generated by peripheral sensory nerve fibres at the brachial plexus, were 37% smaller in hypertensives than normotensives these data suggest that hypertension affects the peripheral nervous system by reducing the number of active sensory nerve fibres without affecting myelination. However, hypertension does not seem to affect the afferent somatosensory pathway within the central nervous system. In sum, hypertension may represent a risk factor for peripheral neuropathy of the sensory nerves.

Buchthal F & Rosenfalck A. (1966). Brain Res 3, 1-122.

Edwards L *et al.* (2008). Psychophysiology 45, 141-147.

Gilliatt RW. (1978). Muscle Nerve 1, 352-359.

Mauguiere F *et al.* (1999). In: Deuschl G, Eisen A, editors. Recommendations for the Practice of Clinical Neurophysiology: Guidelines of the International Federation of Clinical Physiology. Elsevier Science B.V. p. 79-90.

This research and LE was funded by the British Heart Foundation (FS/03/128).

Authors have confirmed where relevant, that experiments on animals and man were conducted in accordance with national and/or local ethical requirements.

PC109

Role of Transient Receptor Potential Vanilloid 1 receptors in C- vs Aδ-fibre-evoked spinal nociception in naïve rats and in a model of post-operative pain

S. Koutsikou[1], E. Davies[1], A. Timperley[1], K. Patel[1], R. Apps[1], J. Palecek[2] and B. Lumb[1]

[1]Physiology and Pharmacology, University of Bristol, Bristol, UK and [2]Functional Morphology, Academy of Sciences of the Czech Republic, Prague, Czech Republic

Transient Receptor Potential Vanilloid 1 (TRPV1) is a cation channel gated by noxious heat, H^+ ions and capsaicin. TRPV1 is sensitised and upregulated in inflammation, and contributes to